Recursive Mode Star Identification Algorithms

MALAK A. SAMAAN
DANIELE MORTARI
JOHN L. JUNKINS
Texas A&M University

Star identification can be accomplished by several different available algorithms that identify the stars observed by a star tracker. However, efficiency and reliability remain key issues and the availability of new active pixel cameras requires new approaches. Two novel algorithms for recursive mode star identification are presented here. The first approach is derived by the spherical polygon search (SP-search) algorithm, here used to access all the cataloged stars observed by the sensor field-of-view (FOV) and recursively add/remove candidate cataloged stars according the predicted image motion induced by camera attitude dynamics. Star identification is then accomplished by a star pattern matching technique which identifies the observed stars in the reference catalog. The second method uses star neighborhood information and a catalog neighborhood pointer matrix to access the star catalog. In the recursive star identification process, and under the assumption of "slow" attitude dynamics, only the stars in the neighborhood of previously identified stars are considered for star identification in the succeeding frames. Numerical tests are performed to validate the absolute and relative efficiency of the proposed methods.

Manuscript received October 6, 2003; revised October 22, 2004; released for publication April 1, 2005.

IEEE Log No. T-AES/41/4/860795.

Refereeing of this contribution was handled by M. Ruggieri.

This work was supported by the Italian Space Agency and the National Aeronautics and Space Administration.

Authors' address: Dept. of Aerospace Engineering, Texas A&M University, H. R. Bright Bldg., Room 741A, 3141 TAMU, College Station, TX 77843-3141, E-mail: (mortari@aero.tamu.edu).

I. INTRODUCTION

Star trackers are widely used for attitude determination in both orbiting and interplanetary spacecraft. The most critical stage of the attitude determination process using a star tracker is the star identification process (star-ID). This is reflected by a wide variety of approaches, well described by existing literature [1–12]. The star-ID problem is a time-consuming process also requiring a large amount of memory for the star catalog. This is why faster techniques are still needed, especially to solve the lost-in-space case, where no attitude information is available.

The introduction of a new concept, the k-vector, to solve the range searching problem without a searching phase (that is dramatically faster than the standard binary search technique), resulted in a substantial step toward faster algorithms to solve the star-ID problem. This method, which has been used and demonstrated effective to access star catalog data [13–14], was then specialized in [15] for its application to different problems requiring range searching. It yields also to the development of new approaches [16–18] to solve the general star-ID problem.

However, the need to solve the lost-in-space case, is a generally rare event in the lifetime of a standard operating star tracker. Most of the time, a star tracker already knows, within some known uncertainties, the three axis attitude. This information is, therefore, very useful to alleviate the heavy star-ID process by reducing the overall star catalog to a small subset of it. The knowledge, even approximate, of the angular velocity vector in both modulus and direction, can also be used to estimate which stars will leave the sensor field-of-view (FOV) and which stars will appear. This operating mode, called recursive mode, is the operating mode in which a high degree of speed is required. In fact, the higher the star tracker frame rate is, the more effective and accurate the control system will be.

Two new very fast algorithms to accomplish the recursive star-ID process (not the lost-in-space case), are presented here. These two methods, which are ideally suited for the emerging active pixel camera technology, are:

1) the spherical polygon search (SP-search) approach. This method, which is derived from [16] and [17], accesses the stars that can potentially lie within the star tracker FOV and then the interstar angles between the measured stars and the cataloged stars are used in a tiered logical algorithm to establish the star-ID.

2) the star neighborhood approach (SNA). This method, which represents an alternative to the SP-search, also accesses candidate stars and performs the star-ID by locating the observed cataloged stars (those falling in the instrument FOV) by a cataloged

knowledge of stars neighboring the identified stars from the previous frame.

To start the recursive mode of the star-ID process, the recently developed "Pyramid" lost-in-space algorithm, presented in [18] (which improves the first version of it, see [19]), is adopted to obtain the initial quaternion and the direction cosine matrix. In Pyramid, the star-ID process is quantified by evaluating the expected random frequencies associated with matching interstar angles from measured star polyhedra.

For each successive frame, the SNA or the SP-search algorithm, as proposed herein, is used to obtain the expected stars in the FOV, from the star catalog. A "hypothesis-test" logical method for star pattern identification, by matching interstar angles in the measured frame to those in the expected stars, completes the star-ID process. The angular velocity can be estimated by using the rate gyro and the quaternion will be integrated at each time t to obtain the direction cosine matrix, although as frame rates increase, it is possible to dispense with gyro measurements for many missions. The attitude estimator adopted in both the proposed algorithms is the second estimator of the optimal quaternion (ESOQ-2, see [20]), that represents an alternative to the first estimator of the optimal quaternion (ESOQ-1 or ESOQ), presented in [21]. The adopted ESOQ-2 version incorporates the improvements described in [22].

The two new recursive star-ID algorithms, presented here, are supported by simulation results.

II. SPHERICAL POLYGON APPROACH

Mortari [16] established the SP-search approach to access and identify stars observed by a wide FOV star tracker. SP-search is used to identify the stars observed by a wide FOV star tracker and uses more than once the k-vector technique [23, 24]. SP-search does not require any (accurate or not) initial guess of the spacecraft attitude, and does not use the typically low accuracy magnitude information. The method uses reference (cataloged) and observed star pairs as the basis on which the star-ID process is accomplished for all of the observed stars. Of course matching a single star pair leads to a large number of ambiguities, however, we find matching a four star pattern virtually eliminates the possibility of ambiguities (for > 5000 candidate stars and $\cong 17$ μrad centroiding precision, the probability of invalid matches of all six interstar angles is on the order of $\sim 10^{-12}$).

The problem to find all the stars admissible with a given direction $\mathbf{w} \equiv \{x, y, z\}^{\mathrm{T}}$ with uncertainty $h\sigma$, that is, all those falling within the cone of axis $\mathbf{w}$ and aperture $h\sigma$, can easily be accomplished using the k-vector technique applied to the three components, x, y, and z, of the catalog stars $\mathbf{r}_k$. In fact, the uncertainty cone of the $\mathbf{w} \equiv \{x, y, z\}^{\mathrm{T}}$ direction implies that the

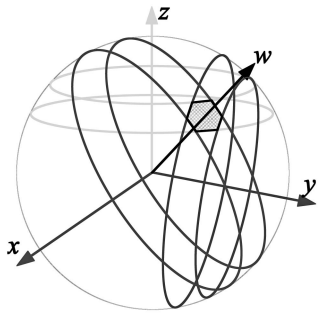

Fig. 1. Spherical polygon.

true component $x_{\mathrm{true}} = \mathbf{x}_{\mathrm{ECI}} \cdot \mathbf{r}_k = \mathbf{r}_k(1)$ must fall within the range

$$x_{\min} \leq x_{\mathrm{true}} \leq x_{\max} \tag{1}$$

where [$s = \sin(h\sigma)$ and $c = \cos(h\sigma)$]

$$\begin{cases} x_{\min} = cx - s\sqrt{1 - x^2} \\ x_{\max} = cx + s\sqrt{1 - x^2} \end{cases} \tag{2}$$

and, similarly for the other two components y_{true} and z_{true} of $\mathbf{r}_k$, within the ranges

$$\begin{cases} y_{\min} \leq y_{\mathrm{true}} \leq y_{\max} \\ z_{\min} \leq z_{\mathrm{true}} \leq z_{\max} \end{cases} \tag{3}$$

where

$$\begin{cases} y_{\min} = cy - s\sqrt{1 - y^2} \\ y_{\max} = cy + s\sqrt{1 - y^2} \\ z_{\min} = cz - s\sqrt{1 - z^2} \\ z_{\max} = cz + s\sqrt{1 - z^2} \end{cases}. \tag{4}$$

The stars satisfying the conditions given in (1) and (3) are distributed in an annular spherical surface identified as the area between the two cones having axis as the $\mathbf{x}$ coordinate axis and with aperture $\cos^{-1}(x_{\min})$ and $\cos^{-1}(x_{\max})$, respectively. Now the admissible stars are all those satisfying all the three different and orthogonal annular spherical surfaces (with respect to all of the three coordinate axes).

Thus, the searched admissible stars are all those falling within the intersection among the three annular spherical surfaces depicted in Fig. 1.

III. STAR NEIGHBORHOOD APPROACH

The autonomous star-ID makes use of the knowledge of the previous frame data to initiate the current frame star-ID. The SNA is introduced as a novel method of using the previously identified stars to access the candidate stars to match with the current measured stars. Fig. 2 shows the representation of the SNA in which the union of the neighborhood of previously identified stars is used as the current estimated star-ID. The radius of the region of the neighbor $\delta\vartheta$ is proportional to the spacecraft angular velocity ω and to the frame rate Δt. Pointers to a cone of neighboring cataloged stars are included in the

TABLE I
Example of Star Neighbor Table of Indices

Star #	$\mathbf{r}_1$	$\mathbf{r}_2$	$\mathbf{r}_3$	$\mathbf{r}_4$	$\mathbf{r}_5$	$\mathbf{r}_6$	$\mathbf{r}_7$	$\mathbf{r}_8$	$\mathbf{r}_9$
3341	4132	4579	4580	4131	2145	1257	712	0	0
3342	4161	3707	1555	902	903	2674	43	2146	435
3343	267	553	95	988	1249	1385	1376	1733	1898
3344	208	237	410	1003	1137	1258	1385	1742	0
3345	4634	4140	4141	4590	3711	1120	433	2972	638
3346	54	60	154	171	205	272	617	0	0
3349	4640	4639	1007	802	909	995	1401	1935	0
3350	4640	3715	3746	4147	1386	1735	1918	1559	619
3352	3354	4676	4644	4643	3353	3750	1403	2391	0
3353	62	804	911	996	1403	2152	2392	2391	2700
3354	4644	3352	2393	437	2700	1739	996	807	0
4140	60	154	205	617	893	4141	3346	3345	2972
4141	60	171	205	617	3345	3712	3711	4140	3346

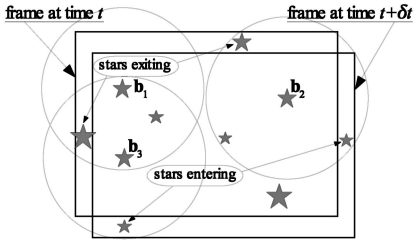

Fig. 2. Star neighborhood.

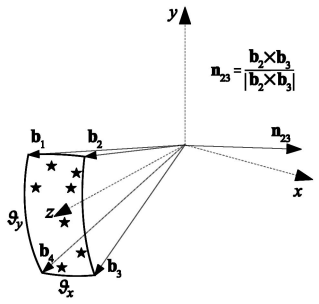

Fig. 3. Sensor's four corners.

mission star catalog, so once a star has been identified we have a search-less method to access all neighbors in a cone centered on that star.

Table I shows a sample data of some stars that have cataloged indices and the corresponding neighbor indices of (pointers identifying) nine neighboring stars in a cone centered on each one of them.

The star neighbor approach depends mainly on the locations of the stars with respect to the star tracker sensor's four corners in the body reference frame. Fig. 3 shows the sensor frame in the body frame.

The sensor frame components of the position vector of the sensor's four corners are

$$\begin{cases} \mathbf{b}_1^{\mathrm{T}} = \{-\sin\vartheta + \cos\vartheta\sin\varepsilon + \cos\vartheta\cos\varepsilon\} \\ \mathbf{b}_2^{\mathrm{T}} = \{+\sin\vartheta + \cos\vartheta\sin\varepsilon + \cos\vartheta\cos\varepsilon\} \\ \mathbf{b}_3^{\mathrm{T}} = \{+\sin\vartheta - \cos\vartheta\sin\varepsilon + \cos\vartheta\cos\varepsilon\} \\ \mathbf{b}_4^{\mathrm{T}} = \{-\sin\vartheta - \cos\vartheta\sin\varepsilon + \cos\vartheta\cos\varepsilon\} \end{cases} \tag{5}$$

where $(\pm\vartheta)$ and $(\pm\varepsilon)$ are the right ascension and declination of the sensor's four corner. We can use the vector dot product to get the relationships

$$\begin{cases} \mathbf{b}_1^{\mathrm{T}}\mathbf{b}_4 = \mathbf{b}_2^{\mathrm{T}}\mathbf{b}_3 = \cos\vartheta_y = \\ \qquad\qquad = \sin^2\vartheta + \cos^2\vartheta(\cos^2\varepsilon - \sin^2\varepsilon) \\ \mathbf{b}_1^{\mathrm{T}}\mathbf{b}_2 = \mathbf{b}_3^{\mathrm{T}}\mathbf{b}_4 = \cos\vartheta_x = \\ \qquad\qquad = -\sin^2\vartheta + \cos^2\vartheta = \cos(2\vartheta) \end{cases} \tag{6}$$

where ϑ_x and ϑ_y are the camera angular FOV in **x** and **y** direction, respectively. Thus, we have

$$\begin{cases} 2\cos^2\vartheta - 1 = \cos\vartheta_x \quad \Longrightarrow \quad \vartheta = \dfrac{\vartheta_x}{2} \\ \cos^2\varepsilon = \dfrac{\cos\vartheta_x + \cos\vartheta_y}{\cos\vartheta_x + 1} \end{cases}. \tag{7}$$

Now, to check that a certain star is found inside the FOV we have to check the angle between the star position vector $\mathbf{b}_k$ and the normal to each side of the star tracker, i.e., if $\mathbf{n}_{ij}$ is the vector normal to the side of the vectors $\mathbf{b}_i$ and $\mathbf{b}_j$ or $\mathbf{n}_{ij} = (\mathbf{b}_i \times \mathbf{b}_j)/\|\mathbf{b}_i \times \mathbf{b}_j\|$ then the star $\mathbf{b}_k$ lies inside the FOV if and only if

$$\begin{aligned} \mathbf{b}_k^{\mathrm{T}}\mathbf{n}_{12} < 0, \qquad \mathbf{b}_k^{\mathrm{T}}\mathbf{n}_{23} < 0 \\ \mathbf{b}_k^{\mathrm{T}}\mathbf{n}_{34} < 0, \qquad \mathbf{b}_k^{\mathrm{T}}\mathbf{n}_{41} < 0. \end{aligned} \tag{8}$$

So, by knowing the attitude matrix at each time step we can calculate the normal vectors to the sensor frame in the body frame. Meanwhile, using (8) and the star catalog, we can simulate the frames of the stars at each time step.

A. Star Identification Algorithm

Once the stars are simulated, using the conditions in (5)–(8), the star neighbor algorithm is used as follows.

1) The recently developed Pyramid LISA algorithm is used [18] to solve the lost-in-space case. The star-ID at time t_0 becomes known.

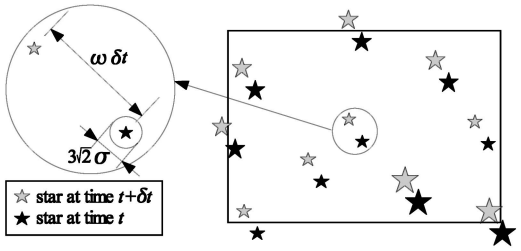

Fig. 4. Stars image displacement due to camera motion.

2) The attitude matrix at each time step will be obtained by introducing the angular velocity. The angular velocity will typically be obtained by using the rate gyro and the quaternion will be integrated at each time t to obtain the direction cosine matrix.

3) Given the sensor attitude matrix $C^{\mathrm{T}} \equiv [\mathbf{x}, \mathbf{y}, \mathbf{z}]$ at time t and the simulated star vectors $\mathbf{b}_i$, $(i = 1, \ldots, n)$. Calculate the star locations (x_i, y_i) by using

$$x_i = -f\frac{\mathbf{x}^{\mathrm{T}}\mathbf{b}_i}{\mathbf{z}^{\mathrm{T}}\mathbf{b}_i}, \qquad y_i = -f\frac{\mathbf{y}^{\mathrm{T}}\mathbf{b}_i}{\mathbf{z}^{\mathrm{T}}\mathbf{b}_i} \tag{9}$$

where f is the camera focal length.

4) The estimated location of star i at the current frame $(x_i, y_i)_{t+\delta t}$ is calculated by adding the location of star i at the previous frame $(x_i, y_i)_t$ and estimated translation of the frame $\omega\delta t$.

5) If the distance between the estimated location of star i $(x_i, y_i)_{t+\delta t}$, and the measured location $(x_i, y_i)_{\text{measured}}$ is less than 3 $(\sqrt{2}\sigma)$ then the star i will have the same ID as in the previous frame. Fig. 4 shows a representation of stars at time $(t + \delta t)$ and at time t.

6) For the unmatched stars from steps 4 and 5 we use the neighborhood matrix (Table I) to identify the stars which enter or exit the sensor frame. In this case all neighbor stars are considered to find which stars entered the current frame.

7) The interstar angle, between the unmatched stars and the star neighbors, is checked to find the ID for the unmatched stars.

The logic for the real time star-ID is shown in Fig. 5.

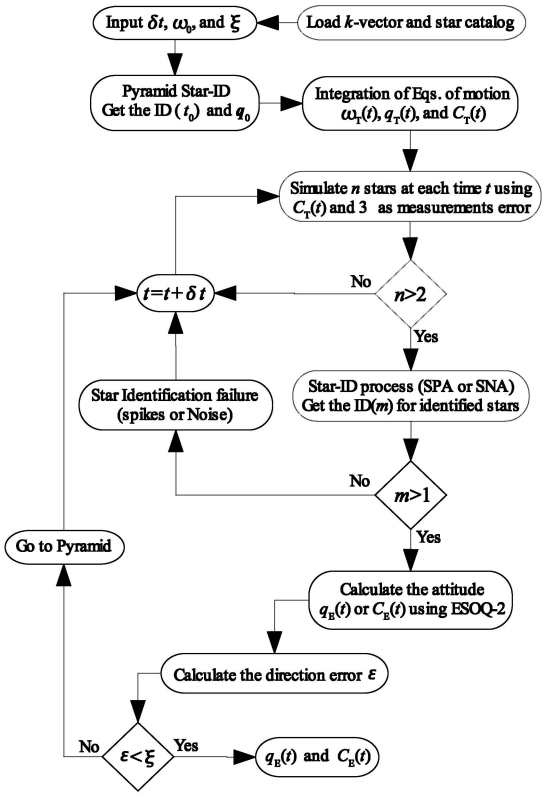

Fig. 5. Logic flow diagram for real time star identification program.

B. Simulation Results

End to end numerical tests, based on simulation of true prescribed attitude motion, star image centroid measurements (including measurement errors), star catalog access, star-ID, and attitude estimation have been carried out. We report here a simulation that is based on a typical 1 h of elapsed real time and using a time step (successive star image frame interval) of $\delta t = 0.1$ s. First, the LISA program is called to solve the lost-in-space problem to estimate the initial attitude with no prior information. The output of this process is the optimal estimate for the quaternion $\mathbf{q}(t_0)$ and the associated direction cosine matrix $C(t_0)$ orienting the camera with respect to the inertial frame in which the cataloged star information is stored. Second, the estimated attitude dynamics is obtained by integrating, between successive times the quaternion kinematics equation

$$\begin{Bmatrix} \dot{q}_1 \\ \dot{q}_2 \\ \dot{q}_3 \\ \dot{q}_4 \end{Bmatrix} = \frac{1}{2}\begin{bmatrix} 0 & \omega_3 & -\omega_2 & \omega_1 \\ -\omega_3 & 0 & \omega_1 & \omega_2 \\ \omega_2 & -\omega_1 & 0 & \omega_3 \\ -\omega_1 & -\omega_2 & -\omega_3 & 0 \end{bmatrix}\begin{Bmatrix} q_1 \\ q_2 \\ q_3 \\ q_4 \end{Bmatrix} \tag{10}$$

together with the angular velocity ω measurements provided by three rate gyros. Then, the star image observation data are simulated using the $C(t)$ and the true known star information from the catalog, together with random numbers to simulate centroiding errors of 17 μrad (1σ).

Fig. 6 shows the histogram of the number of star occurrences for the simulated star measurements. The star-ID procedures are used to identify the stars using either the SP-search or the SNA methods, and of course, the fact that the true attitude and star-ID is known allows us to immediately observe any anomalies in the process.

The overall count of the floating-point operations required are plotted in Fig. 7, as a function of the number of identified stars. Note, due to random measurement errors and other variations, the number

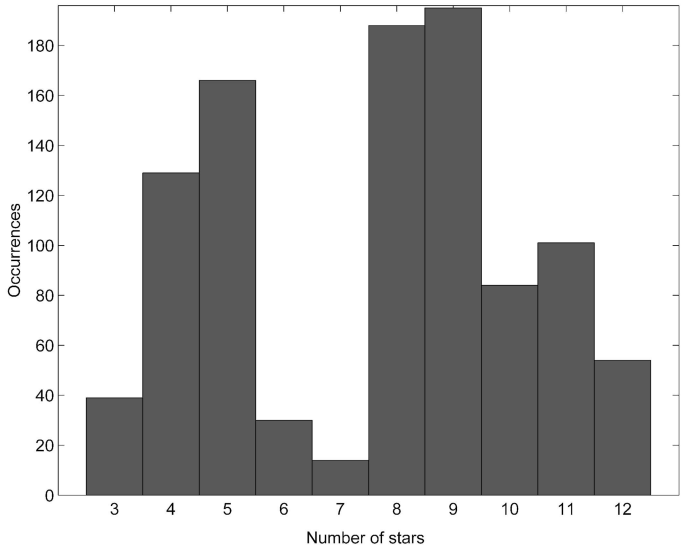

Fig. 6. Histogram of number of star occurrence.

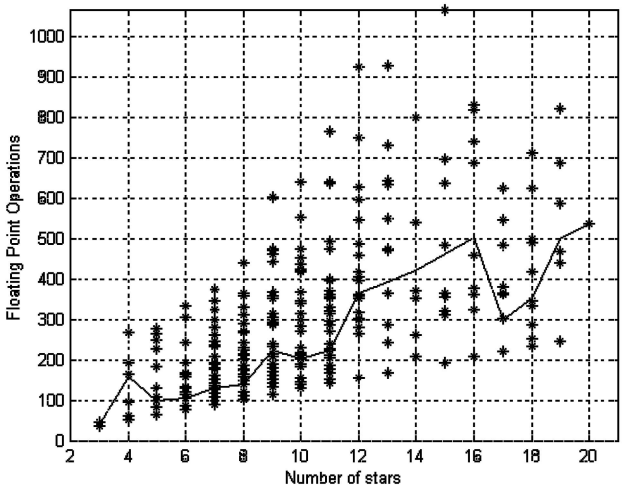

Fig. 7. Floating point operations counts.

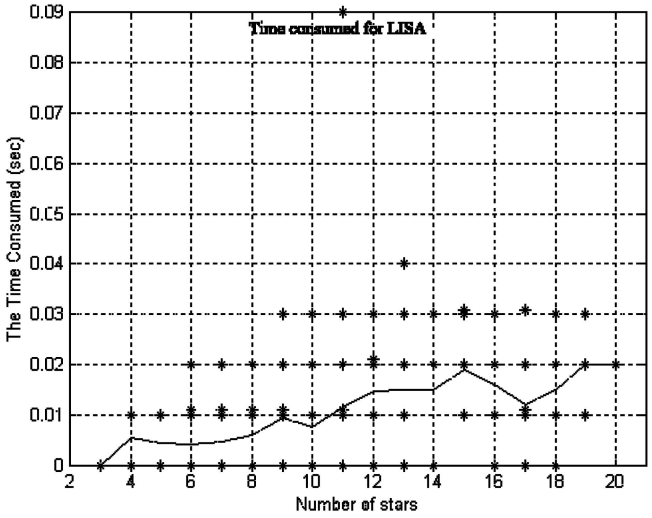

Fig. 8. Consumed time.

of operations is a random variable. All computations were done in MATLAB, and the floating-point operations operator was utilized to obtain the floating-point operation count. As is well known, the floating-point operations count is an imperfect indication of computational load because some logical tests and integer operations are excluded by the floating-point operations calculation. However, the time consumed, using a PC 266MHz operating under Windows 98, is also shown in Fig. 8. This plot gives a more meaningful measure of computational effort that of course can be reduced by over one order of magnitude by utilizing compiled code from, for example, equivalent C-code and an appropriate real time operating system and processor.

Now, by using the fastest available attitude estimator (that is, ESOQ-2 [20], with the latest improvements [22]), the estimated attitude direction cosine matrix $C_{\mathrm{E}}(t)$ is calculated using the observed star vectors and the cataloged star vectors of the identified stars. The parameter that evaluates the maximum "distance" between two orientation matrices (as, for instance, the true and the estimated attitude matrices), is described as the maximum direction error $\varepsilon_{\max}$, that is computed according to

$$\varepsilon_{\max} = \cos^{-1}\left[\frac{\mathrm{trace}(C_{\mathrm{T}}C_{\mathrm{E}}^{\mathrm{T}}) - 1}{2}\right]. \tag{11}$$

now, since the true attitude C_T is always unknown—that implies that the principal axis direction of the attitude corrective matrix $(C_{\mathrm{T}}C_{\mathrm{E}}^{\mathrm{T}})$ is unknown—the "distance" between the true and the estimated attitude matrices, is better described by the expected value

$$E\{\varepsilon\} = \frac{\pi}{4}\varepsilon_{\max}. \tag{12}$$

Fig. 9 shows the expected direction error $E\{\varepsilon\}$ as a function of the number of identified stars. This error is actually polarized about the direction

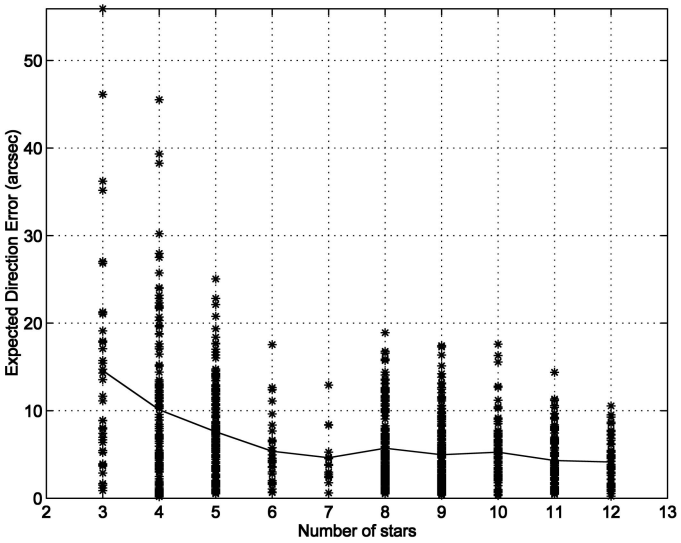

Fig. 9. Expected direction error.

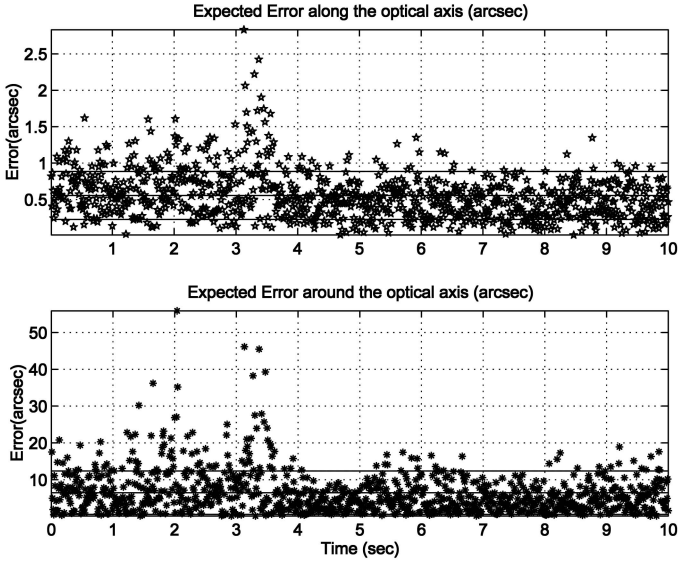

Fig. 10. Expected errors (of and about) optical axis.

of the optical axis **w**. Therefore, the overall error, described by (11), can be decomposed in two parts: ε_a which is associated with the error of **w**, and the remaining part ε_n orthogonal to it. Mathematically, these components are, therefore computed using the following expressions

$$\begin{cases} \cos\varepsilon_a = \mathbf{w}^{\mathrm{T}}\mathbf{w}_{\mathrm{true}} = \mathbf{w}^{\mathrm{T}}(\Delta\mathbf{w}) \\ \cos\varepsilon_n = \mathbf{n}^{\mathrm{T}}\mathbf{n}_{\mathrm{true}} = \mathbf{n}^{\mathrm{T}}(\Delta\mathbf{n}) \end{cases} \tag{13}$$

where **n** indicates any random direction perpendicular to **w** and $\Delta = (C_{\mathrm{T}}C_{\mathrm{E}}^{\mathrm{T}})$. The numerical values of ε_a and ε_n, obtained by numerical tests, are shown in Fig. 10.

IV. SELECTION OF FOV SIZE

The size of the star tracker FOV is one of the most important aspects in the design of the tracker sensor. First, the selection of the FOV size depends on the number of star tracker FOVs. For high accuracy on all three axes, it is well known that at least two star tracker FOVs are required. Second, the important aspect of obtaining a sufficient number of well-separated stars must be properly taken into consideration. In fact, there exist various regions in the celestial sky where the star density substantially differs from the uniform distribution. However, increasing the magnitude threshold implies larger on-board star catalog and slows down the star-ID process. Larger FOVs introduce distortions at the edges. Therefore, tradeoff studies establish to best values for the FOV size and the magnitude threshold.

The probability of finding a certain number of stars is used to plot the FOV size for each threshold magnitude. While the FOV size analysis can be

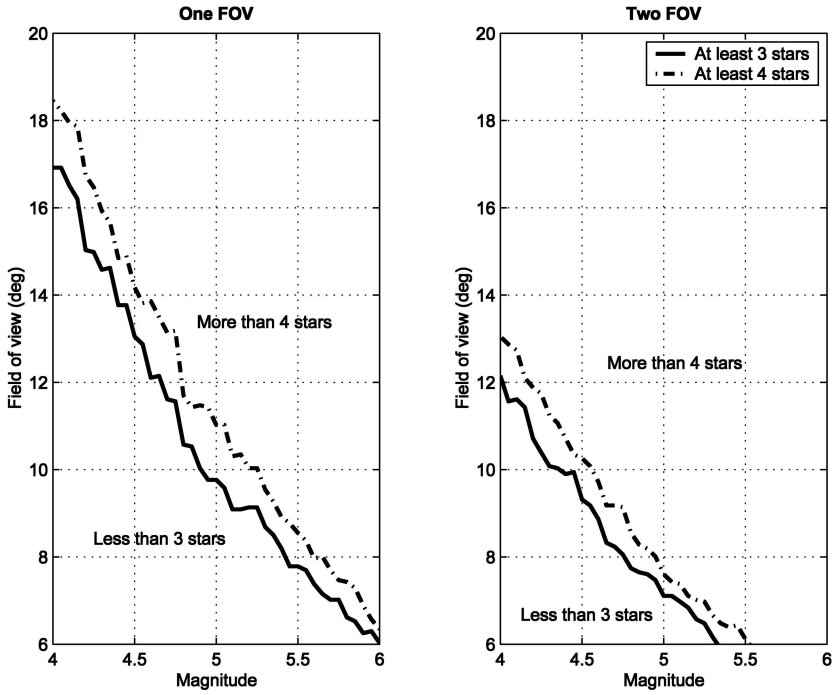

Fig. 11. Selection of FOV size.

approached analytically if we assume uniform star density, it is fairly simple to use the actual star catalog and a simple Monte Carlo process. For each magnitude, 1000 tests have been done to obtain the corresponding FOV size that gives the following probabilities

$$P(\text{No. of stars} < 3) < 0.01$$
$$P(\text{No. of stars} < 4) < 0.01. \tag{14}$$

Fig. 11 shows a plot of the size of square FOV versus the magnitude for magnitude range, (from 4.0 to 6.5), also the same plots are given for two identical star trackers.

V. CONCLUSION

This paper presents two new recursive methods for identifying the stars within the FOV during camera slewing motion. The spherical polygon approach is used to sort the star position vector components in **x**, **y**, and **z**-axes and then the star identification is done by accessing the cataloged stars within the FOV corners and the common stars of each sorted vector in **x**, **y**, and **z** directions.

The SNA is also used as a second method for star identification. In this method we access (without searching) all cataloged stars in the union of the neighborhoods of stars identified in the previous frame. Logic based upon matching the interstar angles between the identified stars and the observed stars provides the final checks.

Finally, we mention that the computational and night-sky experimental validations of the results of this paper were augmented by an on-orbit validation (StarNav I experiment aboard space shuttle Columbia, STS-107, launched on January 2003).

ACKNOWLEDGMENT

We give special thanks to our colleague Thomas Pollock for his numerous discussions of star sensing, star pattern recognition, and spacecraft attitude determination. We sincerely appreciate the contributions of Mike Jacox, David Boyle, and the StarNav team; their support in implementing these concepts in the flight experiment on the STS-107 Columbia mission has been invaluable.

REFERENCES

[1] Junkins, J. L., White, C. C., and Turner, J. D.
Star pattern recognition for real time attitude determination.
Journal of the Astronautical Sciences, **25** (1977), 251–270.

[2] Gunderson, R. W.
Application of fuzzy isodata algorithms to star tracker pointing systems.
In *Proceedings of the Seventh Triennial World Congress*, Helsinki, Finland, June 1978, 1319–1323.

[3] Strikwerda, T. E., and Junkins, J. L.
Star pattern recognition and spacecraft attitude determination.
U.S. Army Engineer Topographic Laboratories, ETL-0260, Fort Belvoir, VA, May 1981.

[4] Singley, M. E.
Pattern recognition for space applications.
NASA-TM-82586, DDF final report, NASA Marshall Space Flight Center, AL, May 1984.

[5] Sasaki, T., and Kosaka, M.
A star identification method for satellite attitude determination using star sensors.
In *Proceedings of the Fifteenth International Symposium on Space Technology and Sciences*, Tokyo, Japan, May 1986, 1125–1130.

[6] Rappaport, B., Dunning, T., Jordan, J., Phillips, K., and Stanton, R.
Autonomous star identification for spacecraft attitude control.
In *Proceedings of the Conference in Astronomy from Large Databases: Scientific Objectives and Methodological Approaches*, Garching, Germany, Oct. 1987, 239–244.

[7] Alveda, P., and San Martin, A. M.
Neural network star pattern recognition of spacecraft attitude determination and control.
In *Advances in Neural Information Processing System I*, Denver, CO, 1988, 314–322.

[8] Strikwerda, T. E., Fisher, H. L., Kilgus, C. C., and Frank, L. J.
Autonomous star identification and spacecraft attitude determination with CCD star trackers.
Spacecraft Guidance, Navigation and Control Systems—First International Conference, held at ESTEC, Noordwijk, The Netherlands, June 4–7, 1991, 195–200.

[9] Liebe, C. C.
Pattern recognition of star constellations for spacecraft applications.
IEEE AES Magazine, **7** (1992), 34–41.

[10] De Antonio, L., Udomkesmalee, S., Alexander, J., Blue, R., Dennison, E., Sevaston, G., and Scholl, M.
Star-tracker based, all-sky, autonomous attitude determination.
SPIE Proceedings, **1949** (1993), 204–215.

[11] Udomkesmalee, S., Alexander, J. W., and Tolivar, A. F.
Stochastic star identification.
Journal of Guidance, Control, and Dynamics, **17**, 6 (Nov.–Dec. 1994), 1283–1286.

[12] Quine, B., and Durrant-Whyte, H. F.
A fast autonomous star acquisition algorithm for spacecraft.
Paper T1-16 of the IFAC Conference on Intelligent Autonomous Control in Aerospace, IACA'95, Aug. 14–16, 1995, Beijing, China.

[13] Mortari, D.
A fast on-board autonomous attitude determination system based on a new star-ID technique for a wide FOV star tracker.
Advances in the Astronautical Sciences, **93**, Pt. II, (1996), 893–903.

[14] Mortari, D.
Search-less algorithm for star pattern recognition.
Journal of the Astronautical Sciences, **45**, 2 (Apr.–June 1997), 179–194.

[15] Mortari, D., and Neta, B.
k-vector range searching techniques.
Paper AAS 00-128 of the 10th Annual AIAA/AAS Space Flight Mechanics Meeting, Clearwaters, FL, Jan. 23–26, 2000.

[16] Mortari, D.
SP-search: A new algorithm for star pattern recognition.
Advances in the Astronautical Sciences, **102**, Pt. II, (1999), 1165–1174.

[17] Mortari, D., and Junkins, L. J.
SP-search star pattern recognition for multiple fields of view star trackers.
Paper 99-437 of the AAS/AIAA Astrodynamics Specialist Conference, Girdwood, AK, Aug. 15–19, 1999.

[18] Mortari, D., Junkins, L. J., and Samaan, M. A.
Lost-in-space pyramid algorithm for robust star pattern recognition.
Paper AAS 01-004 Guidance and Control Conference, Breckenridge, Colorado, Jan. 31–Feb. 4, 2001.

[19] Ju, G., Kim, Y. H., Pollock, C. T., Junkins, L. J., Juang, N. J., and Mortari, D.
Lost-in-space: A star pattern recognition and attitude estimation approach for the case of no a priori attitude information.
Paper of the 2000 AAS Guidance and Control Conference, Breckenridge, CO, Feb. 2–6, 2000.

[20] Mortari, D.
Second estimator of the optimal quaternion.
Journal of Guidance, Control, and Dynamics, **23**, 5 (Sept.–Oct. 2000), 885–888.

[21] Mortari, D.
ESOQ: A closed-form solution to the Wahba problem.
Journal of the Astronautical Sciences, **45**, 2 (Apr.–June 1997), 195–204.

[22] Markley, L. F., and Mortari, D.
New developments in quaternion estimation from vector observations.
In *Proceedings of the Richard H. Battin Astrodynamics Symposium Conference*, vol. 106, Texas A&M University, College Station, TX, Mar. 20–21, 2000, 373–393; paper AAS 00-266.

[23] Mortari, D., Pollock, T. C., and Junkins, J. L.
Towards the most accurate attitude determination system using star trackers.
Advances in the Astronautical Sciences, **99**, Pt. II, (1998), 839–850.

[24] Mortari, D., and Angelucci, M.
Star pattern recognition and mirror assembly misalignment for DIGISTAR II and III star sensors.
Advances in the Astronautical Sciences, **102**, Pt. II, (1999), 1175–1184.

Malak A. Samaan received his B.S. degree from Cairo University, Egypt, and his M.S. and Ph.D. degrees in aerospace engineering, from Texas A&M University, College Station, TX.

He was a research associate with the National Authority for Remote Sensing and Space Sciences (NARSS), Cairo, Egypt, and is currently with the Department of Aerospace Engineering, Texas A&M University. He has been involved in the new generation star tracker StarNav I project, leading to an experiment on the Space Shuttle STS-107. His other interests include orbital mechanics, attitude determination, and spacecraft dynamics and control.

Dr. Samaan is a member of AIAA and AAS.

Daniele Mortari received his Ph.D. in nuclear engineering from La Sapienza University, Rome, Italy, in 1981.

He is currently an associate professor in the Department of Aerospace Engineering, Texas A&M University, College Station, TX. He is active in the fields of orbital mechanics, attitude determination, star navigation, data processing, and matrix analysis.

Dr. Mortari is the author of more than 80 papers. He received the NASA award for the San Marco V mission and the Spacecraft Technology Center award for the StarNav I experiment on the STS-101. He is the Associate editor of the *Journal of the Astronautical Sciences*.

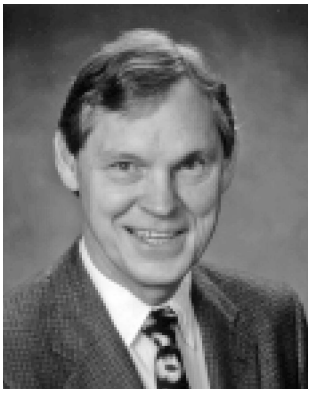

John L. Junkins received his Ph.D. in engineering from UCLA, 1969 (with distinction). He is currently a distinguished professor of the Department of Aerospace Engineering, Texas A&M University, College Station, TX. His research has been implemented in over a dozen space missions and he recently invented the autonomous navigation sensors VisNav and StarNav. He has conducted basic research and led autonomous systems implementations for several space systems, including the StarNav I autonomous navigation experiment (STS 107). He is the Chief Engineer, NASA URETI (TiiMS).

Dr. Junkins has GNC contributions documented in 5 texts, 350 papers, and 5 patents. He is a Fellow of the AIAA.